Earth's Future

RESEARCH ARTICLE
10.1029/2024EF005106

Special Collection:
Regional Sea Level Change and Society

Accounting for Compound Flooding Can Prevent Maladaptation—A Baltic Sea Case Study

Sunna Kupfer[1], Athanasios T. Vafeidis[1], and Leigh R. MacPherson[1]

[1]Department of Geography, Coastal Risks and Sea-Level Rise Research Group, Kiel University, Kiel, Germany

Key Points:

- Ignoring compound flooding in adaptation planning can lead to maladaptation and increased residual risk
- Up from a certain threshold of river discharge, storm surge barriers can lead to an exacerbation of river flooding by up to 100%
- An upstream surge barrier strongly amplifies the flood extent of a hypothetical extreme compound event

Supporting Information:

Supporting Information may be found in the online version of this article.

Correspondence to:

S. Kupfer,
kupfer@geographie.uni-kiel.de

Citation:

Kupfer, S., Vafeidis, A. T., & MacPherson, L. R. (2025). Accounting for compound flooding can prevent maladaptation—A Baltic Sea case study. *Earth's Future*, *13*, e2024EF005106. https://doi.org/10.1029/2024EF005106

Received 18 JUL 2024
Accepted 7 JAN 2025

Abstract Estuarine areas are currently at risk of compound flooding, the frequency and intensity of which is expected to increase with climate change. Even though efforts are made to adapt against single flood drivers using hard protection, potential subsequent changes in flood risk due to compound flooding are often overlooked in flood risk assessments. This is because risk assessments mostly focus on individual flood drivers and do not account for changes in risk from adaptation measures. We address this question and use hydrodynamic modeling to simulate compound flooding for two adaptation scenarios. We consider adaptation in terms of storm surge barriers, in two locations along the Trave estuary, namely Schlutup and Trave, at Lübeck, Germany. We assess the effectiveness of both storm surge barriers in reducing flooding by simulating individual-driver, as well as low- and high-magnitude compound flood scenarios. We find that while during low-magnitude compound flooding both barriers reduce the overall flood extent by 25%–86%, high-magnitude compound flooding leads to an increase of up to 100%, depending on the location of the barrier. Our results suggest that the river contribution is amplified by 52%–100% by the Schlutup Barrier. The Trave Barrier, however, only amplifies flood extents in the high-magnitude compound flood scenarios. Our findings highlight the need to consider compound flooding in adaptation planning to avoid defense failure and unexpected increases in risk. However, as this study considers only two (low probability) extreme events, a more comprehensive approach is necessary to fully understand the overall impact on risk.

Plain Language Summary Particularly in river mouth areas, flooding can be caused by different types of drivers, for example, rainfall, river discharge, or coastal, which can occur simultaneously, leading to extreme flooding. Those combined events are expected to become stronger and more frequent with climate change. Current efforts to protect against flooding often focus on single causes of flooding and do not consider how different types of flooding might interact. This oversight can lead to inadequate protection, where the implementation of single measures can actually increase flood risk. We address this question and investigate compound flooding in Lübeck, Germany, focusing on two storm surge barriers along the Trave estuary. We test these barriers under different flooding scenarios, including individual and combined flooding events. We demonstrate that during smaller combined floods, both barriers can reduce flooding. However, during larger combined floods, flooding can strongly increase due to the implementation of a surge barrier, which can prevent the river from discharging into the estuary, depending on where the barrier is actually located. Our findings highlight the importance of considering all types of flooding when planning flood defenses in order to avoid unexpected additional flooding and ensure effective protection.

1. Introduction

Whether of fluvial, pluvial, oceanic, or combined origin, floods pose a growing threat to low-lying coastal areas in the 21st century, leading to immense damages to coastal infrastructure (EEA, 2023). Without adaptation, the already high and rapidly growing population in low-lying coastal zones—over one-third of the world's population lives within 100 km of the coast (Reimann et al., 2023)—will contribute to increased flooding exposure (MacManus et al., 2021; Reimann et al., 2023; Rentschler et al., 2023). With climate change, the frequency and intensity of hazards affecting the coast is expected to increase globally (Intergovernmental Panel on Climate Change (IPCC), 2022), though with regional and local differences. This spatial variability will result in hotspots in the occurrence of extremes (Kirezci et al., 2020; Myhre et al., 2019; Tebaldi et al., 2021). According to projections by Vousdoukas et al. (2018), the North and Baltic Seas will experience the highest increase in extreme sea levels (ESL) within Europe, which will likely lead to enhanced flooding and subsequent damages over northern Germany (Rutgersson et al., 2022).

Adapting to ESL remains challenging for a number of reasons, including but not limited to economic barriers, the many conflicting interests along the coast (Hinkel et al., 2018), and difficulties in implementing nature-based solutions (Temmerman et al., 2023). As a result, many coastal areas that already experience flooding at a frequent level are sparsely protected. One representative example is the German Baltic Sea coast, of which only 6% is protected by state embankments and 5% by regional dikes (MELUR, 2022; Sterr, 2008). The most recent storm surge which occurred along the German Baltic Sea coast in October 2023 has emphasized this, as it caused comparably high damages and several breaches of regional dikes which generally exhibit a lower protection level than state embankments (MELUR, 2022; NDR, 2023).

To identify where adaptation measures are required, flood risk assessments are a first step and a useful tool to delineate highly exposed areas (Kiesel et al., 2023). A common way to assess local-scale flooding is to simulate flooding using hydrodynamic models (Höffken et al., 2020; Kumbier, Carvalho, Vafeidis, & Woodroffe, 2018; Kupfer et al., 2024; Lyddon et al., 2020; Orton et al., 2023) and to intersect resulting flood characteristics with population or asset data to calculate damage (Hallegatte et al., 2011; Hauer et al., 2021). However, such assessments mostly focus on flooding without potential protection strategies and thus neglect how adaptation measures can change flood risk. Although adaptation is actually considered in broad-scale studies, albeit in a stylized manner (e.g., by assuming defences in densely populated areas) potential and plausible adaptation responses are not commonly considered in local scale studies. Few recent studies performed at local scale have explored the benefits and drawbacks of selected adaptation measures and assessed the respective changes in flood characteristics. Such assessments often include stakeholder involvement in the selection of locally relevant adaptation measures (Louisor et al., 2022; Schroder et al., 2022; Vollstedt et al., 2021). Vollstedt et al. (2021), for example, have selected feasible adaptation measures for their location of interest, but excluded these selected measures from hydrodynamic simulations. Schroder et al. (2022) use a hydrodynamic modeling study to find that while certain adaptation measures protect areas of interest, they can exacerbate flooding elsewhere. This emphasizes the urgency to explore a range of adaptation options in a location-specific manner, due to the variety of coastal morphology, distribution of infrastructure, settlements, or tourist facilities at the coast.

However, flooding is not always due to a single driver but can result from the interaction of multiple drivers of pluvial, fluvial, or oceanic origin. This is commonly referred to as compound flooding (Zscheischler et al., 2018). Compound events can strongly exacerbate flooding, even when neither of the drivers is extreme, compared to the individual occurrence of flood drivers (Bilskie & Hagen, 2018; Kumbier, Carvalho, & Woodroffe, 2018; Kupfer et al., 2022; Olbert et al., 2023). Regional climate projections suggest changes in precipitation patterns and river discharge regimes, which in northern Germany will increase by up to 15%–20% per degree of global warming for the period 2071–2100 (Aalbers et al., 2018; Rutgersson et al., 2022). In combination with a higher frequency of ESL events, this can increase the risk of co-occurrence of flood drivers (Bevacqua et al., 2019).

The increasing likelihood of compound flood events and their potentially disastrous consequences highlight the need to consider compound flooding, not only in flood risk assessments in order to gain a comprehensive understanding of flood risk (Kumbier, Carvalho, Vafeidis, & Woodroffe, 2018; Kupfer et al., 2022; Moftakhari et al., 2019; Ward et al., 2011), but also in coastal protection management and planning (Eilander et al., 2023; van den Hurk et al., 2023; Maymandi et al., 2022; Orton et al., 2023).

Changes in flood characteristics due to the implementation of adaptation measures, especially storm surge barriers in estuaries, can become relevant when different flood drivers co-occur. However, few studies have assessed the effectiveness of selected adaptation measures during compound flood conditions (Eilander et al., 2023; Torres et al., 2015). Orton et al. (2023) identify research gaps regarding the effectiveness and drawbacks of storm surge barriers and suggest that closing storm surge barriers can lead to an accumulation of rainfall or the river. They stress that amongst other challenges this has to be considered in the planning phase of adaptation measures. Moreover, Kumbier, Carvalho, Vafeidis, and Woodroffe (2018) have pointed out that the closure of an estuarine inlet may lead to enhanced flooding, as it prevents high river discharge from flowing into the ocean. These findings reveal that neglecting compound flooding in coastal flood risk assessments and adaptation planning can result in adaptation failure, leading to the need for further exploration of the effectiveness of adaptation measures against compound flood events. This becomes especially relevant in areas where the current probability of compound flooding is low and where future changes in flood drivers due to climate change can cause unexpected compound flood events. In such regions implemented adaptation measures can lead to levee effects and high residual risk (Di Baldassarre et al., 2018). Locations along the German Baltic Sea coast provide a good example,

as both the level of protection (Sterr, 2008) and the current probability of compound flooding are low, but future projections show an increase in compound flood events of 30 days (250–500 days) for RCP2.6 (RCP8.5) between 2070 and 2099 (Heinrich et al., 2023).

Here we address this gap by incorporating a set of structural coastal adaptation measures in a compound flood assessment, using hydrodynamic modeling for the city of Lübeck, located on the German Baltic Sea coast and the Trave River. With the support of stakeholder knowledge, we investigate storm surge barriers as protection measures and explore differences in flood extent under conditions with and without adaptation, and for different flood driver scenarios. We account for one individual river discharge (Q), one individual storm surge (ESL) event, and two compound flood events as flood driver scenarios. We select the 200-year storm surge event, as this return period is used to determine flood protection heights in northern Germany. For Q we account for one historical event and one synthetic high-magnitude event. With the choice of high-magnitude compound flood events we aim to account for low-probability, high-impact scenarios, as these are often underrated in risk assessments and decision-making (Merz et al., 2009; Schumann, 2017). With the use of such an event, we further account for uncertainties of future climate change as the literature suggests increased precipitation for the Baltic Sea region (Aalbers et al., 2018; Heinrich et al., 2023; Rutgersson et al., 2022) and with climate change induced SLR, ESL events may become more frequent and thus more likely in the future (Rutgersson et al., 2022; Vousdoukas et al., 2018). We quantify resulting differences in flood characteristics and discuss those in a location-specific manner to demonstrate that adaptation options can change in effectiveness during compound flooding, compared to coastal flood conditions. In this study, we do not aim to propose protection measures. We rather demonstrate how the effectiveness of adaptation options can be explored and accounted for in a more comprehensive manner in flood risk assessments.

2. Study Area

The Hanseatic city of Lübeck, the second-largest city of Germany's northernmost state Schleswig-Holstein, is located at the Lübeck Bight of the Baltic Sea. The area around Lübeck comprises many low-lying coastal areas. Additionally, the city developed on the banks of the Trave River and an island surrounded by the river, connecting the historic city center to the Baltic Sea. Since 1987 the entire historic city center has been part of UNESCO's World Heritage and therefore holds high cultural and consequently touristic significance (Hansestadt Lübeck, 2022; UNESCO WHC, 2022).

Lübeck's strategic location for trade and today's tourism makes the city susceptible to flooding from both the coast and the River Trave.

Past flooding events have occurred as a result of severe storm surges (peak water levels (WLs) > 1.5 m above mean sea level (MSL)), with the most recent events occurring in 2017, 2019, and October 2023 with peak WLs ranging between 1.74 and 1.78 m (BSH, 2017, 2019, 2023). These events caused minor floods, affecting the historic city center of Lübeck and Travemünde. To date, no engineered coastal flood protection measures exist at Lübeck or Travemünde (Hofstede, 2008), which is generally representative of the protection situation at the Baltic Sea coastline in Schleswig-Holstein (Sterr, 2008). Only dunes along the southern beach of Travemünde protect the Priwall and are thus the only coastal protection in this area. Under the rising pressure of SLR and associated increased probability of storm surges, the city of Lübeck is currently discussing how to effectively adapt to future SLR without compromising the UNESCO World Heritage status, which causes challenges in planning and managing flood protection strategies.

Another source of flooding at Lübeck is flooding caused by the Trave River, although such events are relatively rare. The Trave has its source 25 km north of the city of Lübeck, its total length, however, measures 70 km before it reaches the city. The Trave's total length is 113 km (MUNL SH, 2004). The mean flood discharge at the gauge station Lübeck Moisling is 8 m^3/s, within the period 2004–2024 (HSI-SH, 2024). Even though river flooding at Lübeck is rare, qualitative historical data describe three events in which the Trave River caused major flooding (Bekanntmachungen Lübeck, 1966; Stadtarchiv Lübeck, 1926, 1929). Moreover, on the 4th of January 2024, the gauging station Lübeck Moisling measured a peak discharge of ∼75 m^3/s, making it the second-highest event ever measured (LfU-SH, 2024). At the same time, strong easterly winds caused a storm surge, raising WLs up to 1.50 m in the Trave (BSH, 2024), see also Figure S2 in Supporting Information S1. This led to inundations in parts of Travemünde and Lübeck's historical city center. Such compound flood events are generally considered unlikely at Lübeck because heavy rainfall or long-lasting rainfall events and storm surges are caused by different

10.1029/2024EF005106

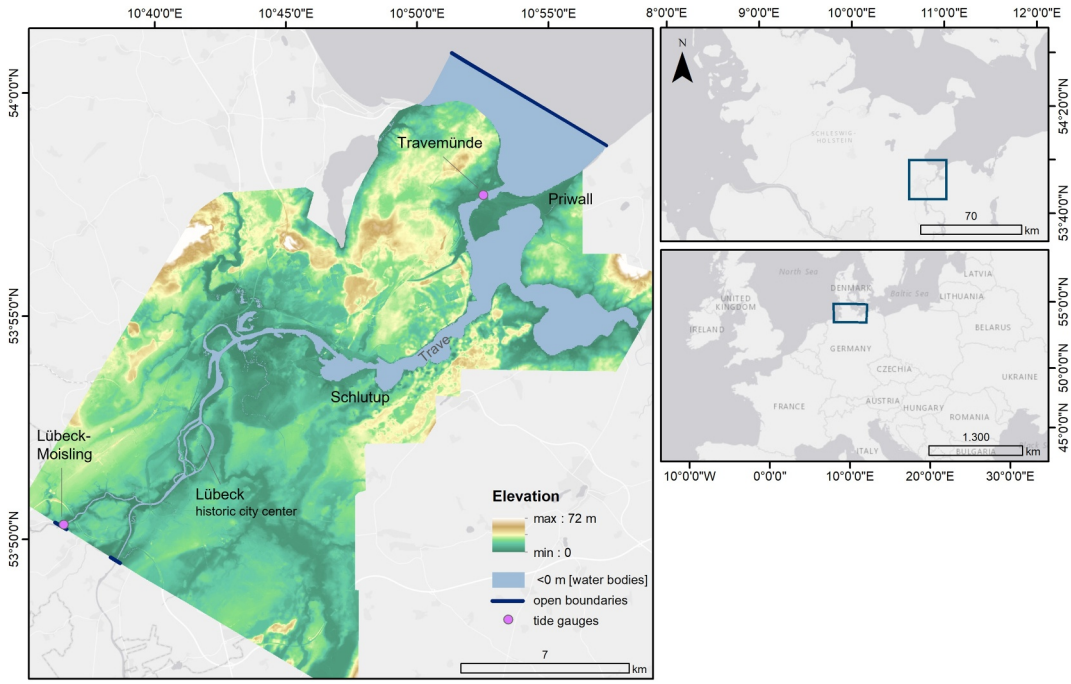

Figure 1. Digital elevation model (DEM) showing the study area of greater Lübeck, at the same time being the model domain. The minimum water depth of water bodies is −20 m, but depth values are not shown here for reasons of visualization. The figure also highlights tide/river gauges and for this study most important locations.

pressure systems. For example, long-lasting rainfall events are generated by westerly winds, transporting moisture from the North Atlantic toward Germany (Ibebuchi, 2022). Storm surges at Lübeck, on the other hand, are commonly produced by strong north-easterly winds, generated by low-pressure systems above the North Sea, moving eastwards and high-pressure systems over Scandinavia and Eastern Europe (BSH, 2024).

However, the last event and findings by Heinrich et al. (2023) along with projections of increasing precipitation by Aalbers et al. (2018) and Rutgersson et al. (2022) suggest that compound flooding at Lübeck may become more relevant in the near future.

3. Methods

3.1. Data and Hydrodynamic Model Description

We simulate compound flooding (CF) from coastal ESL and extreme river discharge (Q) in the area of the lower Trave. This includes the historical city center of Lübeck, the surrounding built-up and industrial areas, as well as Travemünde and the Priwall (Figure 1). We use the fully integrated open-source hydrodynamic model Delft3D (Lesser et al., 2004). Delft3D has been extensively used in coastal and compound flooding applications (Eilander et al., 2023; Kumbier, Carvalho, Vafeidis, & Woodroffe, 2018; Luijendijk et al., 2017; Lyddon et al., 2019). We perform the simulations on a 10 m × 10 m rectangular grid, covering a model domain of 305 km^2, which includes the area of the lower Trave from the river gauge station Lübeck Moisling to the entrance of the Trave in Travemünde, extending into the Baltic Sea. The model set-up has previously been fully calibrated and validated, as described in Kupfer et al. (2024).

For our analysis, we force the model at two open boundaries: the Baltic Sea boundary, with hourly WL time series; and the Trave boundary, with hourly Q. This data is prescribed in terms of ESL and Q hydrographs generated for the compound flood analysis. For the ESL event, we employ the method of MacPherson et al. (2019) to model ESL hydrographs at Travemünde. This allows us to select a hydrograph with a specific return period, which is not available in the observational record. Q observations from the river gauge Lübeck Moisling (LfU-SH, 2024) are used for Q hydrographs. We provide a full event and scenario description in Section 3.2. For further details on the data used, the model set-up, model calibration, and validation, see Kupfer et al. (2024).

3.2. Selection and Generation of ESL and Q Events

Here, we investigate the effect of four different adaptation measures on flood characteristics during compound flooding. This analysis first requires an understanding of the flood characteristics resulting from flood-driver-only scenarios without adaptation. Therefore, we develop four different flood driver scenarios, accounting for ESL and Q. Tides are included in the ESL hydrographs generated by MacPherson et al. (2019), but contribute very little to the shape of each event due to the small tidal range present in the region (Feistel et al., 2008). We have excluded the effect of waves in our analysis as they have relatively low energy in the Baltic Sea and significant wave heights are on average less than 1 m during storm conditions (Bonaduce et al., 2019), due to the constriction of the basin. Moreover, we disregard pluvial flooding, as the hydrodynamic model Delft3D cannot account for this flood driver. Therefore, the four flood driver scenarios include two compound flood events with different magnitudes of Q, one individual ESL event, and one individual Q event.

To develop compound flood scenarios, first, we analyze observed WL and Q time series of the Travemünde and Lübeck-Moisling gauges (see Figure 1) for co-occurring events. We do not estimate driver dependencies or joint-probabilities between river discharge and storm surges, as the river discharge time series is relatively short (22 years). Moreover, Heinrich et al. (2023) have shown no significant dependency at the Trave for today's conditions. However, according to Harrison et al. (2021) and Serafin et al. (2019), the change in flood risk due to compound flooding compared to risk from individual flood drivers does not only depend on the number of co-occurring events but also on the characteristics of estuaries. The tide gauge in Travemünde provides hourly water level (WL) measurements, covering the period 01/11/1949–25/06/2024, by the time we received the data from the water and shipment authorities of Schleswig-Holstein (WSA, 2022). The river gauge Lübeck Moisling measures discharge every 5 min and covers the period of 02/09/2002 19:35 until 25/03/2024 16:00. To be compatible with the hourly resolution of the WL data, we extracted the maximum Q occurring within each hour of the full time-series.

We perform peaks-over-threshold (POT) analysis on both observational time series to identify extreme events (Coles, 2001). For the analysis of ESL, we follow the methodology of MacPherson et al. (2019). First, the WL time series is detrended using a 1-year moving average of mean higher high water (MHHW). This method of detrending is preferred over the use of MSL as it accounts not only for long-term trends, but also seasonal trends (Arns et al., 2013) which have been shown to lead to underestimations if ignored (Allamano et al., 2011). Next, a threshold is set equal to the 97th percentile of peak water levels declustered using a period of 3 days, which ensures that the peak events are independent. Those peak water levels which exceed this threshold are then sampled as ESL. For Q, extremes were sampled using a threshold equal to the 95th percentile of peak Q events. This was chosen as it provides a sufficiently large number of events for our analysis. As with the analysis of ESL, the Q observational data was first detrended using a 1-year moving average of peak Q declustered with a period of 3 days.

From the sample of ESL and extreme Q events and during the period covered by both time series (02/09/2002–25/03/2024), we detect 20 events that co-occur within a time window of 3 days (Couasnon et al., 2018). Among these 20 events, we find two events where one of the drivers (ESL, Q) has a critical magnitude that leads to considerable flooding when occurring individually, while the other driver (Q, ESL) has a magnitude where we expect negligible flooding. However, one event occurred in January 2024, where ESL peaked at 1.47 m, 3 hr before river discharge reached a critical magnitude of 70 m^3/s to cause flooding (Figure S2 in Supporting Information S1). Therefore, we generate artificial compound flood scenarios using a synthetic ESL event, one Q event from the discharge observations, and a second synthetic Q event.

For our storm surge scenario, we use an ESL event with a return period of 200 years, as this is used to define design heights of coastal defenses in Schleswig-Holstein (MELUR, 2022). According to MELUR (2022), a 200-year event corresponds to a peak WL of 2.55 m at Travemünde. We obtain a full ESL hydrograph with the peak WL of a 200-year event using the method developed by MacPherson et al. (2019), which generates synthetic but physically plausible ESL hydrographs. The length of the event covers 114 hr. Storm surges can have a relatively long duration in the Baltic Sea, as they are usually caused by seiches and the absence of tides prevents the storm surge from receding due to the tidal cycle (Jensen & Müller-Navarra, 2008). In the following, we refer to this event as ESL_{200}. We use this event both for the two compound flood scenarios and for an individual ESL event.

We use two extreme Q events to account for the river's contribution to flooding. To obtain a full Q hydrograph, we extract the highest recorded event from the river gauge at Lübeck Moisling (LfU-SH, 2024). This event occurred

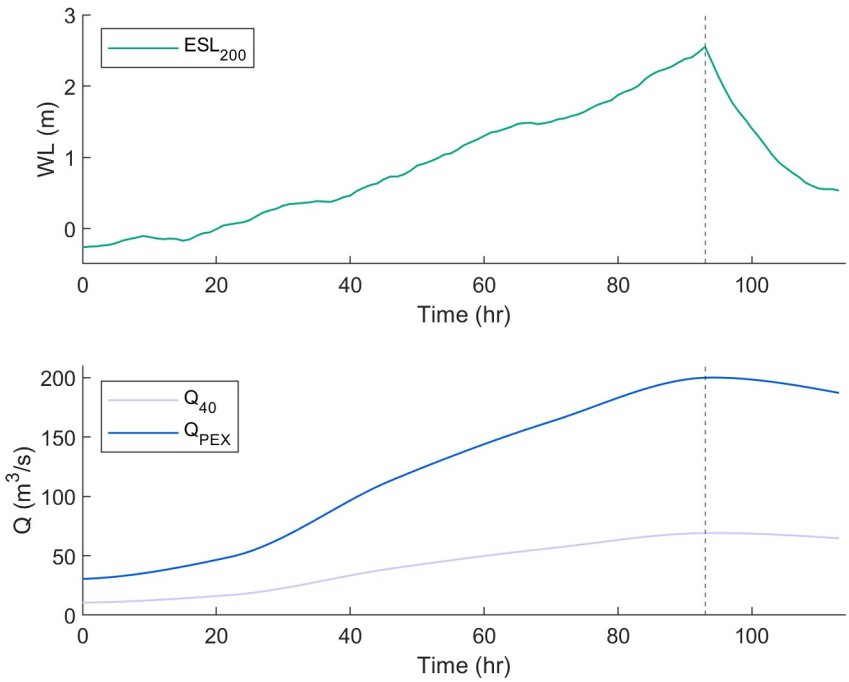

Figure 2. Hydrographs of the three events used as flood driver scenarios in the hydrodynamic model: ESL_{200} (upper panel), Q_{40} (light blue) and Q_{PEX} (dark blue), lower panel. The dashed line crosses the peaks of all events and expresses their co-occurrence during the compound flood simulations.

in December 2014 with a peak discharge of 79.2 m^3/s, lasting 6 days. After an analysis of extremes, we estimate the return period of this event to be ~40 years. We refer to this event as Q_{40}. However, due to the limited availability of river discharge data (less than 22 years), uncertainties at high return periods are large. Despite this, the estimated return periods of Q serve as indicators of the relative Q-event strengths. To estimate return periods, a Generalized Pareto (GP) distribution is fitted to the extreme Q-events sampled using the POT method described above. To account for uncertainties of Q-events not included in the time series and for uncertainties of climate change induced future river discharge events (Aalbers et al., 2018), we consider an event with a peak discharge of 200 m^3/s. This corresponds to a return period of >10,000 years, though with large uncertainties due to the short discharge record (see Figure S1 in Supporting Information S1). Therefore, we refer to this event as Q_{PEX} for "Plausible EXtreme." To generate an artificial future extreme Q event, we normalize the hydrograph of the previously extracted observed event and multiply the normalized hydrograph by 200 m^3/s. When simulating this event individually, we ensure that WLs from the Baltic Sea do not cause any additional flooding. Therefore, we keep the WL time series during this event at a range of 0.1–0.3 m. To ensure that both Q events cover the same length as ESL_{200} (114 hr), we set the start- and endpoint of the Q events accordingly. We end the simulations at the end of the ESL event, even though river discharge is still at a high magnitude. However, storm surge barriers are usually reopened once ESL drop and recede, which prevents river discharge from accumulating any further. Figure 2 shows all three events (ESL_{200}, Q_{40}, Q_{PEX}). For the hydrodynamic flood simulations, we assume that during compound scenarios Q- and ESL-peaks occur at the same time. From those events, we come up with two individual flood driver scenarios: ESL_{200} and Q_{PEX}. We simulate those events individually to demonstrate how compound flooding and the implementation of barriers modify individual driver flood extents. The two compound flood driver scenarios are: $ESL_{200} + Q_{40}$, $ESL_{200} + Q_{PEX}$.

3.3. Development of Coastal Adaptation Scenarios

We developed coastal adaptation scenarios in close co-operation with the City of Lübeck, in the context of a DFG (German Research Foundation) funded research project. Here, a comprehensive flood risk assessment was performed, accounting for deep uncertainty in economic decision analysis (Kupfer et al., 2024; Völz et al., 2024). In this context, we co-organized a stakeholder workshop together with the City of Lübeck in February 2022. Participants were employees of Lübeck's city administration, municipal enterprises, and state enterprises that are

involved in the city's water management and flood prevention. The workshop aimed to capture opinions of the participants on three different topics: (a) Future development of the City of Lübeck and its townscape, (b) realistic and unrealistic coastal adaptation options and strategies, and (c) the period of SLR that should be taken into account for coastal risk management.

The discussion on adaptation options and strategies revealed that the participants considered barriers at narrow parts of the Trave River with complementary dikes or dunes to be the most conceivable and therefore interesting for investigation. We must note that this outcome does not imply that the stakeholders involved actually favor or support the implementation of such measures. Taking into account these potential options discussed during the stakeholder workshop, we developed three main adaptation options: (a) A storm surge barrier at the Trave entrance (Trave) with complementary dikes, (b) a storm surge barrier located at the center of the model domain (Schlutup) with complementary dikes, and (c) sea wall, or dike like protection structures along the Trave and built-up areas.

However, we did not consider the third option, as according to Völz et al. (2024) protection structures at Lübeck exhibit the lowest efficiencies in terms of costs. Moreover, we do not anticipate any additional effect on the flood extent during compound flooding with this measure. Nevertheless, we develop two additional adaptation scenarios, in which we remove the complementary dikes from each storm surge barrier. We do this to gain a more comprehensive understanding of changing flood characteristics during compound flood conditions, as without complementary dikes, flood waves from both flood drivers can flow around the barriers. This process has resulted in four adaptation options, that we consider in this study:

a) A storm surge barrier at Schlutup, upstream (Figure 3a).
b) A storm surge barrier at Schlutup with complementary dikes along built-up and low-lying areas (Figure 3b).
c) A storm surge barrier in Travemünde at the Trave entrance, downstream (Figure 3c).
d) A storm surge barrier at the Trave entrance with complementary dikes, along the Baltic Sea shore of Travemünde and the Priwall (Figure 3d).

We refer to the adaptation measures as follows: (a) S (Schlutup Barrier) (b) SD (Schlutup Barrier with complementary dikes) (c) T (Trave Barrier), and (d) TD (Trave Barrier with complementary dikes). To implement the selected adaptation options in the hydrodynamic model, we increase the pixel height of the underlying digital elevation model (DEM) to the desired adaptation height at the locations of the measures. We chose an adaptation height of 4.70 m to ensure that neither of the flood drivers (ESL and Q) can overflow the protection structure (see Figure S4 in Supporting Information S1). To ensure that the adaptation options are well represented in the DEM, we manipulate the value of the DEM at each pixel that represents the location of the adaptation option. Therefore, the adaptation options have a minimum width of one pixel (10 m). We assume that the barriers remain closed throughout the entire duration of the simulations (length of the ESL event). As storm surges in the Baltic Sea have a comparably long duration due to the negligible tidal signal (see Section 3.2), a closure throughout the entire simulations is reasonable.

Last, we combine the individual ESL scenario (ESL_{200}) and the two compound flood scenarios ($ESL_{200} + Q_{40}$, $ESL_{200} + Q_{PEX}$), described in Section 3.2 with each adaptation measure. We exclude the individual Q_{PEX} scenario from the analysis with adaptation, as this scenario serves as a reference scenario for comparison. Additionally, we aim to analyze the effect of coastal adaptation during compound flooding. In reality, these barriers would therefore only be closed during storm surges, but not during river floods. This results in 16 scenarios, summarized in Table 1. Since we only change the magnitude of Q in the compound flood scenarios, we name the compound flood scenarios according to the Q magnitude (e.g., CF_{40}, CF_{PEX}). We refer to the scenarios for which we exclude adaptation (flood drivers only) as "No Adaptation" scenarios.

4. Results

To explore the effect of adaptation measures against storm surges and compound events, we simulate flooding for each of the 16 developed scenarios, including the individual storm surge (ESL_{200}) and high-magnitude river scenario (Q_{PEX}), which serve as reference scenarios. We compare the flood extents of flood-driver-only scenarios ESL_{200}, Q_{PEX}, CF_{40}, and CF_{PEX} (No Adaptation) with the flood extents resulting from the corresponding adaptation scenario. Each flood extent we are depicting and analyzing here (Figures 4–6) is the maximum flood extent, corresponding to the time step where the largest number of pixel, above the threshold 0 m is flooded.

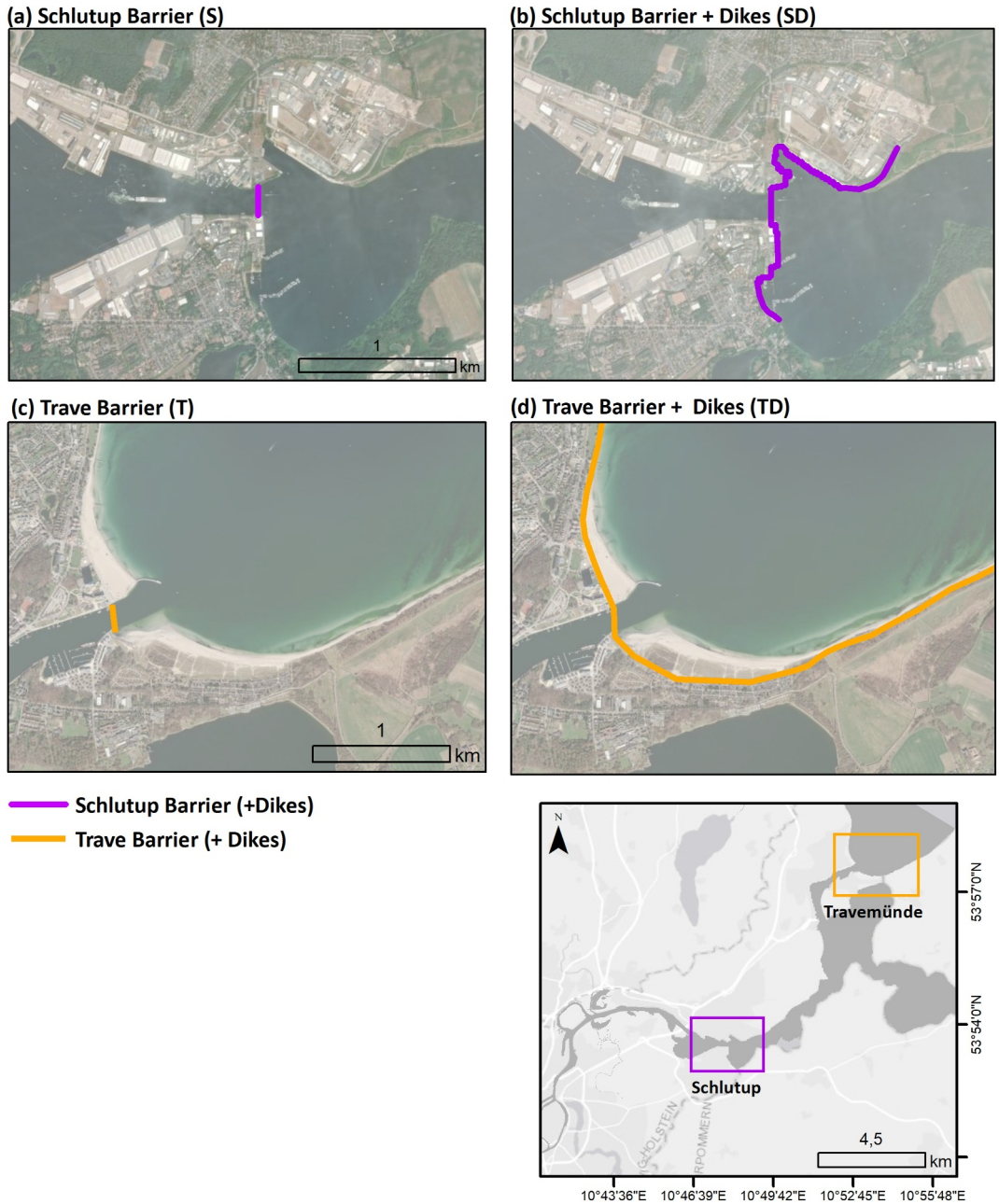

Figure 3. Selected coastal adaptation options in Schlutup (a, b) and Travemünde (c, d). The overview shows where the adaptation options are located in the area of greater Lübeck.

4.1. Individual- and Compound Flood Extents Without Adaptation

First, we analyze differences in flood extents resulting from the scenarios without adaptation, which represent today's state of Lübeck. This analysis is fundamental for further understanding the effect of each adaptation measure. Without adaptation and when flood drivers occur individually, we find that ESL_{200} is the primary flood driver, while flooding caused by Q is minor. The bars in Figure 4a show flood extents resulting from these scenarios (ESL_{200} and Q_{PEX}). While the individual Q event (Q_{PEX}, green) only causes negligible flooding (~1.8 km^2) even at a very high stage, the individual storm surge (ESL_{200}, turquoise) causes a flood extent of ~10.7 km^2, propagating upstream beyond the city center of Lübeck and reaching the upstream boundary of our model domain. We show the individual ESL_{200} flood extent in Supporting Information S1 (Figure S3a). Also

10.1029/2024EF005106

Table 1
Scenario Description

Scenario name	Flood driver	Adaptation measure
ESL_{200}	200-year ESL	No Adaptation
$ESL_{200}S$	200-year ESL	**S** Schlutup Barrier
$ESL_{200}SD$	200-year ESL	**SD** Schlutup Barrier + Dikes
$ESL_{200}T$	200-year ESL	**T** Trave Barrier
$ESL_{200}TD$	200-year ESL	**TD** Trave Barrier + Dikes
CF_{40}	200-year ESL + 40-year Q	No Adaptation
$CF_{40}S$	200-year ESL + 40-year Q	**S** Schlutup Barrier
$CF_{40}SD$	200-year ESL + 40-year Q	**SD** Schlutup Barrier + Dikes
$CF_{40}T$	200-year ESL + 40-year Q	**T** Trave Barrier
$CF_{40}TD$	200-year ESL + 40-year Q	**TD** Trave Barrier + Dikes
Q_{PEX}	extr. Q	No Adaptation
CF_{PEX}	200-year ESL + extr. Q	No Adaptation
$CF_{PEX}S$	200-year ESL + extr. Q	**S** Schlutup Barrier
$CF_{PEX}SD$	200-year ESL + extr. Q	**SD** Schlutup Barrier + Dikes
$CF_{PEX}T$	200-year ESL + extr. Q	**T** Trave Barrier
$CF_{PEX}TD$	200-year ESL + extr. Q	**TD** Trave Barrier + Dikes

during compound flooding with low- and high-magnitude Q contributions (CF_{40}, violet and CF_{PEX}, blue) the effect of Q is minor. In CF_{40} the flood extent is only 0.1 km^2 larger and in CF_{PEX} only 0.2 km^2 is added to the flood extent of ESL_{200}.

4.2. The Effect of the Schlutup Barrier Without and With Complementary Dikes

Second, we analyze the effect of the Schlutup Barrier with and without complementary dikes, which is located at the center of the model domain. To visualize the spatial distribution of all CF flood extents and their differences, which we quantify in Figure 4, we overlay flood extents in the form of flood maps in Figure 5. We find that while the Schlutup Barrier effectively reduces flood extents of ESL_{200} (see turquoise bar in Figures 4a and 4b and flood maps in Figures S3b and S3c in Supporting Information S1) and CF_{40}, it increases flooding of CF_{PEX}. Considering high-magnitude Q_{PEX} occurring individually, however, demonstrates that the river contribution is exceeded by the Schlutub Barrier in both CF scenarios, CF_{40} and CF_{PEX}. Moreover, while in ESL_{200} and CF_{40} the complementary dikes have no additional effect, they amplify the flood in CF_{PEX} even further.

The turquoise bars of Figure 4a (No Adaptation) and b (S) show a reduction of the flood extent of $ESL_{200}S$ by 5.5 km^2 (52.9%), compared to ESL_{200}. We can observe a similar effect in the low-magnitude CF scenario ($CF_{40}S$), where the Schlutup Barrier reduces the total flood extent by 2.1 km^2 (24.9%), compared to CF_{40} under No Adaptation. Figure 5a shows results of CF scenarios with the Schlutup Barrier compared to the CF scenarios under No Adaptation. The map supports the results of Figure 4 but also highlights locations where flood extents differ. The differences between $CF_{40}S$ (violet) and CF_{40} (light blue) occur exclusively west (i.e., landwards) of the Schlutup Barrier. This reveals that a barrier at Schlutup prevents the flood wave produced by ESL from entering the area behind the barrier.

In contrast to the results of the individual ESL_{200} and the low-magnitude CF scenario, the high-magnitude CF scenario, $CF_{PEX}S$ (Figure 4a, dark blue), leads to an increase of 2.9 km^2 (27%) in flood extent compared to CF_{PEX} (Figure 4a, mid blue). The dark blue extent in Figure 5a demonstrates that CF_{PEX} exceeds the flood extent of all

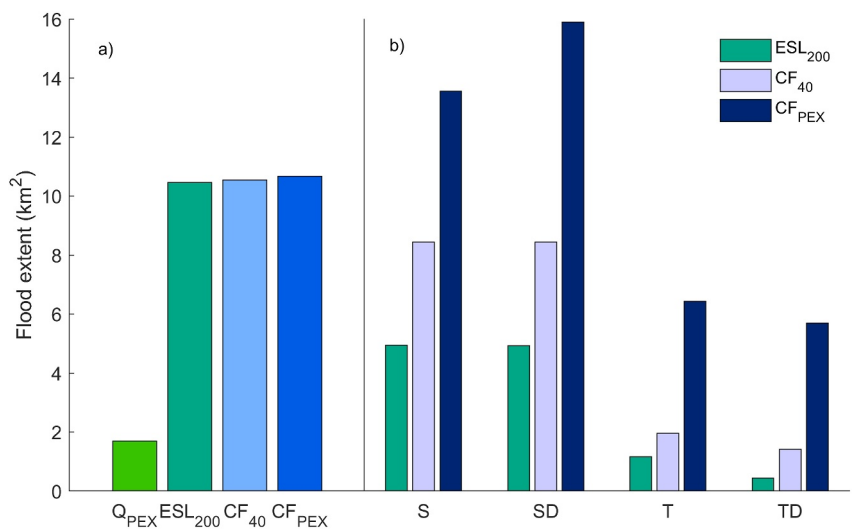

Figure 4. Comparison of flood extents resulting from individual high-magnitude river flooding (Q_{PEX}), individual ESL (ESL_{200}), and compound flooding (CF_{40}, CF_{PEX}) for each of the No Adaptation scenarios (a) and flood driver scenarios together with explored coastal adaptation options (b).

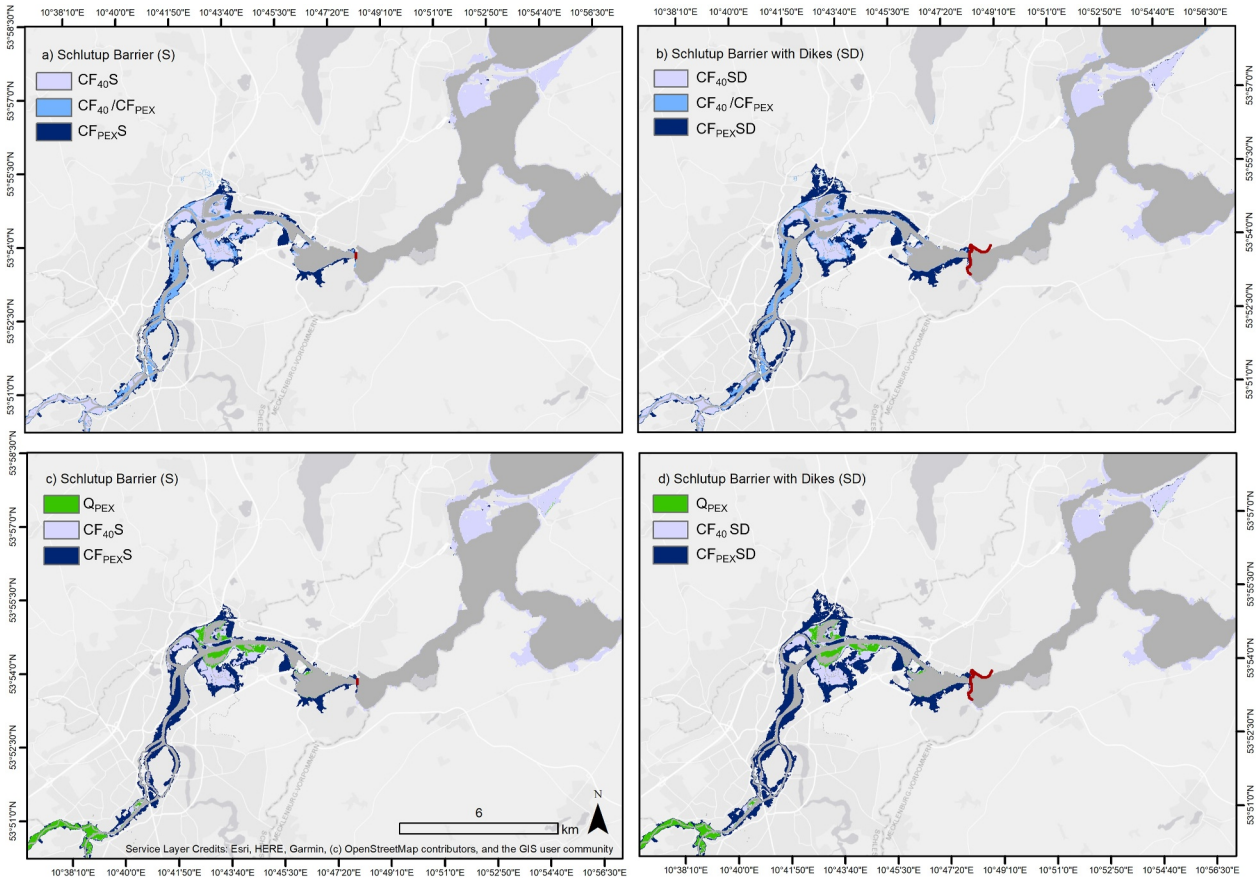

Figure 5. Flood extents resulting from scenarios with the Schlutup Barrier S and the Schlutup Barrier with complementary dikes SD. In panel (a) we show compound flood extents with the barrier, $CF_{40}S$, and $CF_{PEX}S$ (in panel (b) with complementary dikes, $CF_{40}SD$ and $CF_{PEX}SD$) compared to No Adaptation compound flooding (CF_{40}/CF_{PEX}). We show No Adaptation compound flood extents (CF_{40}/CF_{PEX}) as one (light blue) since differences are not visible. In panel (c) we compare compound flood extents with the Schlutup barrier $CF_{40}S$, $CF_{PEX}S$ (in panel (d) with complementary dikes, $CF_{40}SD$, $CF_{PEX}SD$) with the river only scenario Q_{PEX} (green). The order of each legend corresponds to the order of the flood extents (top = smallest extent, bottom = largest extent). The smaller flood extents cover the areas flooded by the larger flood extents.

scenarios, even of the high-magnitude scenario under No Adaptation (CF_{PEX}, mid blue) exclusively west (i.e., landwards of the Schlutup Barrier).

Additionally, we compare flood extents of the two CF- and adaptation scenarios ($CF_{40}S$ and $CF_{PEX}S$) with the flood extent of the individual Q scenario, Q_{PEX} (Figure 5c). As shown previously in Figure 4, the contribution to flooding of Q_{PEX} is relatively small. Figure 5c shows that the Q_{PEX} flood extent (green) only inundates areas behind the barrier. In this area, the flood extents of $CF_{40}S$ and $CF_{PEX}S$ exceed that of Q_{PEX} by 52% and 80% respectively. As we have shown that the ESL contribution is blocked by the barrier, the larger flood extents of the compound flood scenarios, in particular $CF_{40}S$, compared to Q_{PEX} demonstrate an amplifying effect of the Schlutup Barrier during compound flooding.

Further, we consider the Schlutup Barrier with complementary dikes, (SD in Figures 4b, 5b, and 5d). The flood extents in Figure 4b—S compared to SD—and those shown in Figures 5a and 5c, compared to Figures 5b and 5d, demonstrate that in the high-magnitude CF scenarios the complementary dikes have an additional effect. The maximum flood extent of $CF_{PEX}SD$ is 2.3 km^2 (17.3%) larger than $CF_{PEX}S$. Thus, it is substantially larger (5.3 km^2) than the CF scenario without adaptation (CF_{PEX}).

4.3. The Effect of the Trave Barrier Without and With Complementary Dikes

Last, we analyze the effect of the Trave Barrier without and with the addition of complementary dikes on the flood extents during compound flooding. Our results show that the Trave Barrier effectively reduces flood extents in all

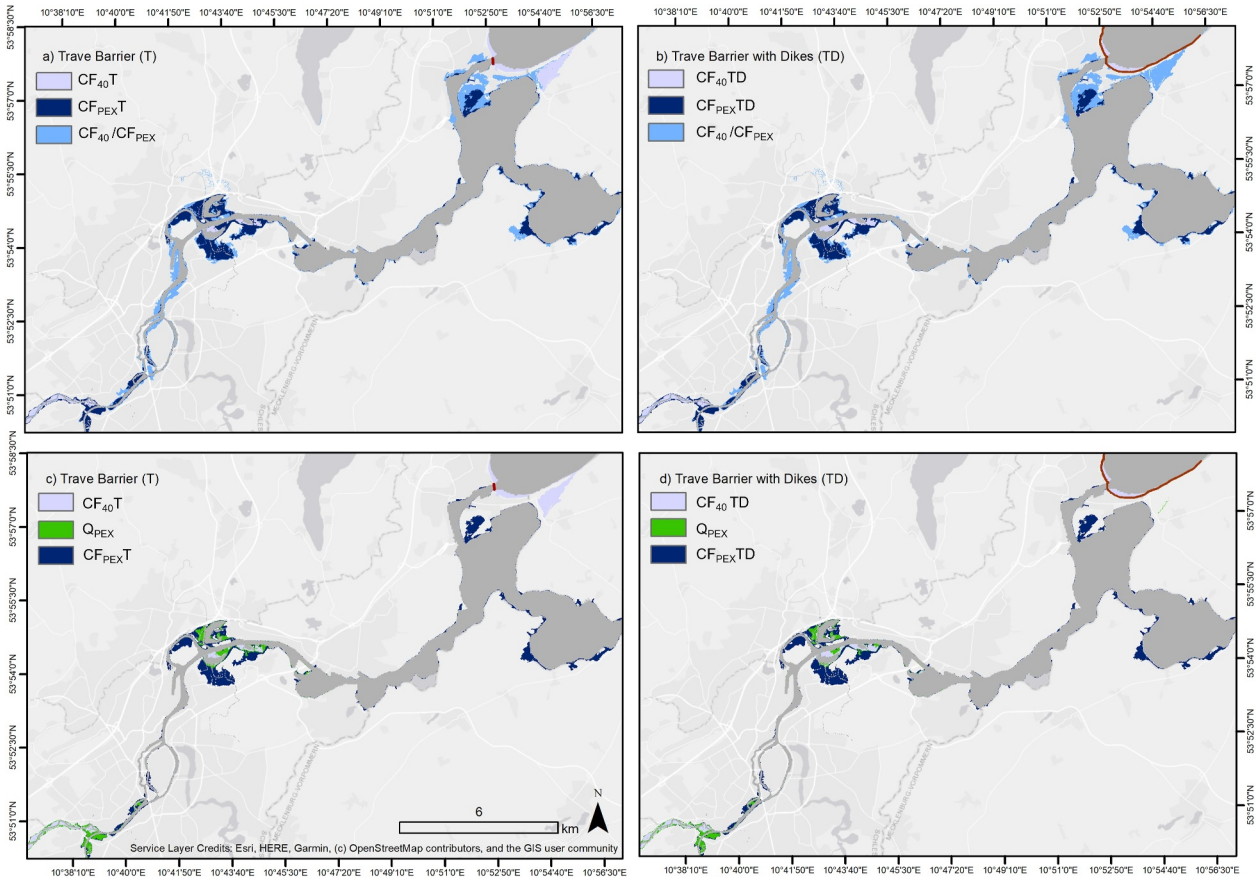

Figure 6. Flood extents resulting from scenarios with the Trave Barrier T and the Trave Barrier with complementary dikes TD. In panels (a) and (b) we show compound flood extents with the barrier, $CF_{40}T$ and $CF_{PEX}T$, ($CF_{40}TD$ and $CF_{PEX}TD$) compared to No Adaptation compound flooding (CF_{40}/CF_{PEX}). We show No Adaptation compound flood extents (CF_{40}/CF_{PEX}) as one (light blue) since differences are not visible. In panels (c) and (d) we compare compound flood extents with the Trave Barrier $CF_{40}T$, $CF_{PEX}T$ (and complementary dikes, $CF_{40}TD$, $CF_{PEX}TD$) with the river only scenario Q_{PEX} (green). The order of each legend corresponds to the order of the flood extents (top = smallest extent, bottom = largest extent). The smaller flood extents cover the areas flooded by the larger flood extents.

scenarios, when ESL_{200} occurs individually and in all CF scenarios (Figure 4 and see also Figures S3d and S3e in Supporting Information S1 for individual flood maps of ESL_{200}). A further reducing effect is achieved when complementary dikes are used. In contrast to results of the Schlutup Barrier, individual Q flooding is reduced in the low-magnitude CF scenario ($CF_{40}T$ (TD)), but amplified in the high-magnitude CF scenario ($CF_{PEX}T$ (TD)).

The groups of bars T and TD in Figure 4 show flood extent comparisons resulting from the scenarios with the Trave Barrier (T) and Trave Barrier with complementary dikes (TD). Again, we support the results of Figure 4 by spatial flood maps in Figure 6.

First, the flood extents of $ESL_{200}T$ and $ESL_{200}TD$ compared to ESL_{200}, No Adaptation (see Figure 4) demonstrate the flood-reducing effect of the Trave barriers. Moreover, comparing the flood sizes of CF_{40} No Adaptation with $CF_{40}T$ (TD) we find a substantially smaller flood extent in $CF_{40}T$ (TD) with differences of 8.5 km^2 (81.4%) and 9.1 km^2 (86.5%) respectively. Considering the coastward side of the Trave Barrier, the map of the $CF_{40}T$ flood extent (Figure 6a, violet) shows that ESL_{200} contributes by a large share to the flood extent in this adaptation scenario. This is shown by the inundated low-lying coastal areas around the Trave Barrier. Those inundated surfaces are disconnected from the Trave, by higher elevated areas. In the scenarios with the complementary dikes, the dikes entirely prevent the ESL_{200} from entering the Trave and low-lying areas (Figure 6b, violet extent in front of the adaptation measure), leading in total to a smaller inundated surface in this area, compared to $CF_{40}T$.

Considering the river contribution in the landward area behind the barrier, unlike the scenario $CF_{40}S$, with the Schlutup Barrier, in both $CF_{40}T$ and $CF_{40}TD$ scenarios, the river contribution does not reach the Trave Barrier (Figures 6c and 6d, violet extent). In both scenarios, the flood extent behind the Trave Barrier is even smaller than

the individual Q flood (Q_{PEX}), 96% in $CF_{40}T$ and 60% in $CF_{40}TD$. Therefore, during low-magnitude CF, the Trave Barrier has no amplifying effect, as the river flooding dissipates before reaching the barrier.

Last, the high-magnitude CF scenarios with the Trave Barrier ($CF_{PEX}T$ and $CF_{PEX}TD$, dark blue extents in Figures 6b and 6d) produce smaller flood extents than CF_{PEX} (No Adaptation, mid blue extent), with differences of 4.24 km^2 (39.7%), and 4.9 km^2 (46.5%). Both scenarios, however, exceed the flood extent of the river-only scenario (Q_{PEX}), by ∼68% and cause major additional floods even far upstream. Therefore, with high-magnitude river discharge, the Trave Barrier substantially amplifies the flood resulting from the river contribution during compound flooding.

5. Discussion

In this study we use hydrodynamic modeling to quantify differences in flood extent by exploring a set of adaptation measures—namely storm surge barriers combined with dikes—during compound flooding, and flooding from storm surge and river discharge occurring individually. Since coastal flood risk assessments typically do not account for (a) potential coastal adaptation and (b) compound flooding, uncertainties remain regarding the effectiveness of adaptation measures in reducing flood extent (Louisor et al., 2022; Schroder et al., 2022), but also regarding the extent to which potential adaptation options can alter or even exacerbate flood characteristics during compound flooding (Kumbier, Carvalho, Vafeidis, & Woodroffe, 2018; Kumbier, Carvalho, & Woodroffe, 2018).

The first outcome that is relevant for the following interpretation of our results is that storm surge is the major flood driver at Lübeck, as it propagates both as individual flood driver (Figure S3 in Supporting Information S1) and in combination with Q far inland. Preliminary tide gauge analyses (Figure S2 in Supporting Information S1) have shown that during a compound event, ESL lead to a drop in Q upstream. However, once the storm surge recedes, Q reaches its peak. Thus, the flood contribution of Q is comparably low. This finding is further supported by general observations from stakeholders, who note that the Trave rarely causes flooding in Lübeck (Hansestadt Lübeck, 2024).

The implementation of a Schlutup Barrier, with or without dikes, and low-magnitude CF ($CF_{40}S$ and $CF_{40}SD$), substantially reduces the total flood extent compared to CF_{40} under No Adaptation. On the one hand, this reduction is achieved by the previously described full blocking of ESL by the Schlutup Barrier from entering the Trave behind the barriers. On the other hand, the Q-contribution in $CF_{40}S$ (SD) does not accumulate behind the barrier to an extent that it exceeds CF_{40} without adaptation. Nevertheless, the comparison of the $CF_{40}S$ (SD) scenarios with the individual Q_{PEX} scenario in the area landward of the barrier reveals an amplification of the Q-contribution during compound flooding, by more than half that of Q_{PEX}.

The high-magnitude compound flood scenarios have shown contradictory results. Here, both compound flood extents under No Adaptation are exceeded by the scenarios with the Schlutup Barrier, just like the individual Q_{PEX} flood extent. Thus, the Q-contribution is strong enough to accumulate to an extent that exceeds the CF_{PEX} extent without adaptation. Moreover, while in the low-magnitude $CF_{40}SD$ scenario, the complementary dikes have no additional effect, in $CF_{PEX}SD$ additional dikes amplify the flood extent compared to $CF_{PEX}S$. We can explain this additional effect based on the flood maps shown in Figures 5 and 6 and Figure S3 in Supporting Information S1. As the high-magnitude river discharge reaches the dikes, an even higher amount of water accumulates behind the structures, resulting in strong backwater effects that enhance the flood. In the low-magnitude CF scenarios, the Q-contribution does not reach the dikes, and the additional reinforcing effect does not occur. Figure S4 in Supporting Information S1 further demonstrates that river discharge does not overflow or surround the Schlutup Barrier in any of the scenarios $CF_{40}S$, $CF_{40}SD$, $CF_{PEX}S$, and $CF_{PEX}SD$, as shown by the identical WL time series (Figure S4 in Supporting Information S1, lower panel) supporting the explanation that additional dikes lead to a stronger accumulation in the worst-case CF scenario (Figure S4 in Supporting Information S1, upper panel).

From the interpretation of our results with the Schlutup Barrier, we derive two main findings. First, our results show that the Schlutup Barrier not only changes compound flood extents, but amplifies them. Especially the amplification of the low-magnitude river discharge contribution during compound flooding ($CF_{40}S$ (SD)), exceeding the flood extent caused by the individual high-magnitude river scenario (Q_{PEX}) is a relevant finding. It clearly demonstrates that neglecting compound flooding in coastal adaptation planning can lead to a considerable underestimation of risk and to an unexpected amplification of residual risk or levee effects. According to Reimann

et al. (2023) and Di Baldassarre et al. (2018) residual risk or levee effects can result from structural protection measures, as they create a false sense of safety and attract migration into the flood plain. This, in turn, can increase the exposure to flooding in protected areas in the event of failure. For the Schlutup Barrier, flood risk would be underestimated if compound flooding were neglected when planning this adaptation measure.

Second, our results suggest a threshold of the Q-magnitude beyond which the Schlutup Barrier strongly amplifies the flood extent, so that it exceeds compound flooding without adaptation. We derive this from the fact that flood extents from low-magnitude compound flooding with adaptation scenarios do not exceed the low-magnitude compound flood extent without adaptation, whereas the flood extents from high-magnitude compound flooding with the Schlutup Barrier can nearly double high-magnitude compound flood extends without adaptation. Such a threshold has two major implications for coastal management and supports the ongoing discussion about the urgency to assess flood risk in a more comprehensive manner (Kupfer et al., 2024; Toimil et al., 2020; Ward et al., 2011) to account for uncertainty. First, determining this threshold requires exploration of a large number of compound flood events. Such a threshold may have large implications for coastal managers and decision makers in terms of for example, evacuation planning or the decision on a discharge level at which a barrier should remain open in the case of a forecasted flood event. Yet, identifying this threshold is beyond the scope of this study.

Moreover, the indication of a threshold beyond which the compound flood extent with a barrier is strongly exacerbated supports the ongoing discussion to account for high-impact low-probability events in flood risk assessments (Hinkel et al., 2015; Merz et al., 2009; Najafi et al., 2024; Schumann, 2017). Throughout our analysis, we consider such extreme events, amongst which one event is exceptionally large. By choosing this event, we aim to explore flooding under very extreme conditions while at the same time accounting for future changes in precipitation and thus river discharge, as projected by Heinrich et al. (2023), Aalbers et al. (2018), and Rutgersson et al. (2022), which can lead to higher magnitude and more frequent compound flood events (Bevacqua et al., 2019). Accounting for future changes in precipitation, but also SLR, is particularly relevant when it comes to planning adaptation measures, as these should be designed for long-term protection (Haasnoot et al., 2013). The increasing likelihood of a compound flood event to occur in Lübeck, in combination with our results, further highlights the relevance of including compound flooding into the adaptation planning process for estuaries where the current likelihood of compound flooding is low.

Beyond the Schlutup barrier, we also consider a second location for a storm surge barrier at the entrance of the Trave, namely the Trave Barrier. In the scenarios with the Trave Barrier (with or without dikes), neither the low-magnitude nor the high-magnitude CF scenarios exceed the flood extent of the compound flood scenarios under No Adaptation. Additionally, the flood extents of both low-magnitude compound flood scenarios are smaller than the extent caused by the high-magnitude individual Q-scenario. These results differ greatly from those of the Schlutup Barrier and can be attributed to the fact that the Trave Barrier is located at the river mouth, that is, very far downstream. This location allows the Q-contribution sufficient space to dissipate before reaching the barrier. Also, the flood extents resulting from the high-magnitude compound flood scenarios with the Trave Barrier differ greatly from the results with the Schlutup Barrier. Even though the high-magnitude Q-contribution does reach the Trave Barrier, which blocks and amplifies the flood extent of the Q-contribution, this occurs to a much smaller extent, compared to the results with the Schlutup Barrier. In the scenarios with the Trave Barrier, the high-magnitude Q-contribution exceeds the flood extent of the individual Q-scenario but it remains smaller than the high-magnitude CF extent without a barrier.

The effect of the Trave Barrier across almost all scenarios indicates that the Trave Barrier is the more effective coastal adaptation solution in terms of reducing flood extent. Even though Völz et al. (2024) have estimated that the Trave Barrier is more expensive than the Schlutup Barrier, they have also shown that, during individual storm surge conditions, the Trave Barrier with complementary dikes is more efficient than the Schlutup Barrier. Thus, from a perspective that focuses solely on protection, the city of Lübeck may opt for the downstream Trave Barrier. However, without the consideration of compound flooding, the city of Lübeck may still opt for the Schlutup Barrier for economic and logistical reasons. The study of Völz et al. (2024) does not account for the national and international shipping traffic of high economic value that departs and arrives at a harbor in Travemünde inside the Trave River on a daily basis. In light of the long duration of storm surge events in the Baltic Sea, a closure of a Trave Barrier may therefore imply large economic losses for the city of Lübeck. Moreover, between the harbor and the location of the Schlutup Barrier the primary landuse type is agricultural land or forest and most of the industrial areas, larger settlements, and, above all, the historic city center are located upstream of the Schlutup

Barrier. Therefore, our findings have large implications for the planning process of structural protection measures, not only for Lübeck and the Trave Estuary. Communities along other estuaries may prefer such measures further upstream due to for example, topographic conditions, land occupation or wide estuary entrances. SLR poses another relevant aspect, when considering storm surge barriers as adaptation measure. As Orton et al. (2023) point out, SLR will lead to higher frequencies of barrier closures and longer closure times of barriers, which may have implications for the results of our study, as it increases the likelyhood of river discharge accumulating behind closed barriers. Considering this, however, is beyond the scope of our study.

Moreover, our study contains three major limitations. First, given the short length of the observational Q-record, we cannot estimate joint-probabilities and return periods for Q-events higher than the maximum observed events, without producing large uncertainties (MacPherson et al., 2023; Pugh, 2004). Second, better understanding the effect of storm surge barriers during compound flooding would require a more comprehensive analysis, such as the consideration of a wider range of compound flood events, including estimates of their probabilities. A third limitation is that we are only assessing changes in flood extent and do not analyze flood depths and exposure to compound flooding. However, assessing exposure is beyond the scope of our study and should be accounted for in future research.

Last, we must note that we are not aiming to suggest or recommend the analyzed coastal adaptation measures. The decision for specific adaptation measures requires the consideration of many factors such as for example, port operations, UNESCO World Heritage Sites, surrounding land use, ecological aspects, and estuarine or coastal morphological characteristics. Moreover, other than structural protection measures there is a wide range of alternative adaptation options, including nature-based solutions (NbS), or hybrid approaches of structural measures combined with NbS (Narayan et al., 2016; Schoonees et al., 2019). While structural protection measures can have drawbacks (Bongarts Lebbe et al., 2021), NbS are often considered more sustainable than structural protection measures and are of high ecological value (Sutton-Grier et al., 2015).

6. Conclusions

Our results highlight that storm surge barriers can substantially amplify flood extent during compound flooding. Even though river discharge is a minor flood driver at Lübeck, both barriers and complementary dikes lead to an increase in river discharge induced flooding during low- and high-magnitude compound flooding. However, the amount of amplification of the flood extent depends strongly on the magnitude of the flood driver, and the location of the storm surge barrier. For the upstream barrier, the Schlutup Barrier, our results suggest the existence of a threshold above which the flood extent is increased to an extent to exceed total compound flood extents. Defining this threshold has implications for the barriers operating times and emergency planning, but requires further analysis which is beyond the scope of this study.

These results demonstrate that neglecting compound flooding in coastal adaptation planning can lead to a considerable underestimation of risk and an unexpected increase in residual risk. In light of climate change, this becomes particularly relevant for efficient long-term adaptation planning. The current probability of compound flooding with co-occurring storm surges and river discharge, where both drivers are at an extreme stage, is relatively low at Lübeck. Yet, this probability may increase due to climate change. Hence, we conclude that compound flooding should be accounted for when planning hard coastal protection measures, even in estuarine areas with currently low compound flood probability. In such regions, there is little understanding of possible compound flood impacts, which can even lead to an increase in levee effects in those areas protected by structural measures. Further, the suggested threshold of the flood extent amplification emphasizes the need to account for high-impact low-probability events in order to comprehensively assess flood risk.

The downstream Trave Barrier, shows an amplification of flood extents only during high-magnitude compound flooding. This suggests that this barrier is the more efficient adaptation measure. We must note, however, that the aim of our study is not to recommend a specific protection measure for the city of Lübeck, but rather to explore the effect of measures on compound flooding. In this context we only consider two hard protection strategies; nevertheless, there is a large variety of alternative adaptation options, that should be explored in terms of efficiency in future research. Moreover, our analysis only explores two compound flood events and capturing the full extent of possible consequences during compound flooding would require exploring a larger number of events, the analysis of additional flood characteristics such as flood depths or flood timings, and, depending on the location of the considered estuary other possible flood drivers being waves or heavy precipitation.

Data Availability Statement

The hydrodynamic model Delft3D version 4.04.01, developed by Deltares and in this study used for the simulation of flood extents was downloaded from the Deltares Website (DELTARES, 2018). Bathymetric data can be downloaded at ELC INSPIRE (GeoSeaPortal, 2024). Landuse data (CLC, 2018) are available through the Copernicus Land Monitoring Service. Digital elevation model data (DGM5) were requested from State Office for Surveying and Geoinformation (LvermGEO, 2023). WL and Q Hydrographs for the model calibration and validation were requested from the local Water and Shipment Authorities (WSA, 2022), as well as the State Office for the Environment (HSI-SH, 2024; LfU-SH, 2024). All WL and Q hydrographs used as model input to produce flood extents of individual flood drivers and compound events as well as shapefiles of the adaptation measures are available on figshare (see Kupfer, 2025).

Acknowledgments

All data used in this paper are properly cited and referred to in the reference list. We acknowledge the data provision of WL and Q records for scientific purposes of the Federal Maritime and Hydrographic Agency (BSH), the local Water and Shipment Authorities (WSA, 2022) and the State Office for the Environment of Schleswig-Holstein (LfU). Moreover, we acknowledge the State Office for Surveying and Geoinformation for the provision of topographic data used in the hydrodynamic model (LvermGEO, 2023). This research received funding from the German Research Foundation (DFG) under the SEASCAPEII project as part of the Special Priority Program (SPP)-1889 "Regional Sea Level Change and Society." Open Access funding enabled and organized by Projekt DEAL.

References

Aalbers, E. E., Lenderink, G., van Meijgaard, E., & vanden Hurk, B. J. J. M. (2018). Local-scale changes in mean and heavy precipitation in Western Europe, climate change or internal variability? *Climate Dynamics*, *50*(11–12), 4745–4766. https://doi.org/10.1007/s00382-017-3901-9

Allamano, P., Laio, F., & Claps, P. (2011). Effects of disregarding seasonality on the distribution of hydrological extremes. *Hydrology and Earth System Sciences*, *15*(10), 3207–3215. https://doi.org/10.5194/hess-15-3207-2011

Arns, A., Wahl, T., Haigh, I. D., Jensen, J., & Pattiaratchi, C. (2013). Estimating extreme water level probabilities: A comparison of the direct methods and recommendations for best practise. *Coastal Engineering*, *81*, 51–66. https://doi.org/10.1016/j.coastaleng.2013.07.003

Bevacqua, E., Maraun, D., Vousdoukas, M. I., Voukouvalas, E., Vrac, M., Mentaschi, L., & Widmann, M. (2019). Higher probability of compound flooding from precipitation and storm surge in Europe under anthropogenic climate change. *Science Advances*, *5*(9), 1–8. https://doi.org/10.1126/sciadv.aaw5531

Bilskie, M. V., & Hagen, S. C. (2018). Defining flood zone transitions in low-gradient coastal regions. *Geophysical Research Letters*, *45*(6), 2761–2770. https://doi.org/10.1002/2018GL077524

Bonaduce, A., Staneva, J., Behrens, A., Bidlot, J.-R., & Wilcke, R. A. I. (2019). Wave climate change in the North Sea and Baltic Sea. *Journal of Marine Science and Engineering*, *7*(6), 166. https://doi.org/10.3390/jmse7060166

Bongarts Lebbe, T., Rey-Valette, H., Chaumillon, É., Camus, G., Almar, R., Cazenave, A., et al. (2021). Designing coastal adaptation strategies to tackle sea level rise. *Frontiers in Marine Science*, *8*, 740602. https://doi.org/10.3389/fmars.2021.740602

BSH. (2017). Sturmflut vom 04./05.01.2017. Retrieved from https://www.bsh.de/DE/THEMEN/Wasserstand_und_Gezeiten/Sturmfluten/_Anlagen/Downloads/Ostsee_Sturmflut_20170104.pdf;jsessionid=EA4C46DE05D4153900C304EC4F236ED1.live11291?__blob=publicationFile&v=6

BSH. (2019). Sturmflut vom 02.01.2019. Retrieved from https://www.bsh.de/DE/THEMEN/Wasserstand_und_Gezeiten/Sturmfluten/_Anlagen/Downloads/Ostsee_Sturmflut_20190102.pdf?__blob=publicationFile&v=5

BSH. (2023). Schwere Sturmflut vom 20.Oktober 2023. Retrieved from https://www.bsh.de/DE/THEMEN/Wasserstand_und_Gezeiten/Sturmfluten/_Anlagen/Downloads/Ostsee_Sturmflut_20231020.pdf?__blob=publicationFile&v=5

BSH. (2024). Sturmflut an der deutschen Ostseeküste (03.01.2024 und 04.01.2024). Retrieved from https://www.bsh.de/DE/THEMEN/Wasserstand_und_Gezeiten/Sturmfluten/_Anlagen/Downloads/Ostsee_Sturmflut_20240103.pdf?__blob=publicationFile&v=2

CLC. (2018). CORINE land cover 2018 (vector/raster 100 m), Europe, 6-yearly [Dataset]. Retrieved from https://land.copernicus.eu/pan-european/corine-land-cover/clc2018

Coles, S. (2001). *An introduction to statistical modeling of extreme values*. Springer.

Couasnon, A., Sebastian, A., & Morales-Nápoles, O. (2018). A copula-based Bayesian network for modeling compound flood hazard from riverine and coastal interactions at the catchment scale: An application to the Houston Ship Channel, Texas. *Water*, *10*(9), 1190. https://doi.org/10.3390/w10091190

DELTARES. (2018). Downloads [Software]. Retrieved from https://oss.deltares.nl/web/delft3d/downloads

Di Baldassarre, G., Kreibich, H., Vorogushyn, S., Aerts, J., Arnbjerg-Nielsen, K., Barendrecht, M., et al. (2018). Hess Opinions: An interdisciplinary research agenda to explore the unintended consequences of structural flood protection. *Hydrology and Earth System Sciences*, *22*(11), 5629–5637. https://doi.org/10.5194/hess-22-5629-2018

EEA. (2023). European environmental agency: Economic losses from weather- and climate-related extremes in Europe. Retrieved from https://www.eea.europa.eu/en/analysis/indicators/economic-losses-from-climate-related

Eilander, D., Couasnon, A., Sperna Weiland, F. C., Ligtvoet, W., Bouwman, A., Winsemius, H. C., & Ward, P. J. (2023). Modeling compound flood risk and risk reduction using a globally applicable framework: A pilot in the Sofala province of Mozambique. *Natural Hazards and Earth System Sciences*, *23*(6), 2251–2272. https://doi.org/10.5194/nhess-23-2251-2023

Feistel, R., Naush, G., & Wasmund, N. (2008). *State and evolution of the Baltic Sea, 1952–2005: A detailed 50-year survey of meteorology and climate, physics, chemistry, biology, and marine environment*. Wiley-Interscience.

GeoSeaPortal. (2024). ELC_INSPIRE [Dataset]. Retrieved from https://data.bsh.de/SpatialData/Main/ELC_INSPIRE/

Haasnoot, M., Kwakkel, J. H., Walker, W. E., & ter Maat, J. (2013). Dynamic adaptive policy pathways: A method for crafting robust decisions for a deeply uncertain world. *Global Environmental Change*, *23*(2), 485–498. https://doi.org/10.1016/j.gloenvcha.2012.12.006

Hallegatte, S., Ranger, N., Mestre, O., Dumas, P., Corfee-Morlot, J., Herweijer, C., & Wood, R. M. (2011). Assessing climate change impacts, sea level rise and storm surge risk in port cities: A case study on Copenhagen. *Climatic Change*, *104*(1), 113–137. https://doi.org/10.1007/s10584-010-9978-3

Hansestadt Lübeck. (2022). Statistische Nachrichten Nr (p. 50). Retrieved from https://www.luebeck.de/de/rathaus/verwaltung/statistik/index.html

Harrison, L. M., Coulthard, T. J., Robins, P. E., & Lewis, M. J. (2021). Sensitivity of estuaries to compound flooding. *Estuaries and Coasts*, *45*, 1250–1269. https://doi.org/10.1007/s12237-021-00996-1

Hauer, M. E., Hardy, D., Kulp, S. A., Mueller, V., Wrathall, D. J., & Clark, P. U. (2021). Assessing population exposure to coastal flooding due to sea level rise. *Nature Communications*, *12*(1), 1–9. https://doi.org/10.1038/s41467-021-27260-1

Heinrich, P., Hagemann, S., Weisse, R., & Gaslikova, L. (2023). Changes in compound flood event frequency in northern and central Europe under climate change. *Frontiers in Climate*, *5*, 1227613. https://doi.org/10.3389/fclim.2023.1227613
Hinkel, J., Aerts, J. C. J. H., Brown, S., Jiménez, J. A., Lincke, D., Nicholls, R. J., et al. (2018). The ability of societies to adapt to twenty-first-century sea-level rise. *Nature Climate Change*, *8*(7), 570–578. https://doi.org/10.1038/s41558-018-0176-z
Hinkel, J., Jaeger, C., Nicholls, R. J., Lowe, J., Renn, O., & Peijun, S. (2015). Sea-level rise scenarios and coastal risk management. *Nature Climate Change*, *5*(3), 188–190. https://doi.org/10.1038/nclimate2505
Höffken, J., Vafeidis, A. T., MacPherson, L. R., & Dangendorf, S. (2020). Effects of the temporal variability of storm surges on coastal flooding. *Frontiers in Marine Science*, *7*, 1–14. https://doi.org/10.3389/fmars.2020.00098
Hofstede, J. (2008). Coastal flood defence and coastal protection along the North Sea Coast of Schleswig-Holstein.
HSI-SH. (2024). Pegel-Lübeck-Moisling. Retrieved from https://hsi-sh.de/pegel/pegel.html?mstnr=114461
Ibebuchi, C. C. (2022). Patterns of atmospheric circulation in Western Europe linked to heavy rainfall in Germany: Preliminary analysis into the 2021 heavy rainfall episode. *Theoretical and Applied Climatology*, *148*(1–2), 269–283. https://doi.org/10.1007/s00704-022-03945-5
Intergovernmental Panel on Climate Change (IPCC). (2022). *The ocean and cryosphere in a changing climate: Special report of the intergovernmental panel on climate change* (1st ed.). Cambridge University Press. https://doi.org/10.1017/9781009157964
Jensen, J., & Müller-Navarra, S. H. (2008). Storm surges on the German Coast. *Die Küste*, *74*(74), 92–124. ICCE.
Kiesel, J., Lorenz, M., König, M., Gräwe, U., & Vafeidis, A. T. (2023). Regional assessment of extreme sea levels and associated coastal flooding along the German Baltic Sea coast. *Natural Hazards and Earth System Sciences*, *23*(9), 2961–2985. https://nhess.copernicus.org/articles/23/2961/2023/
Kirezci, E., Young, I. R., Ranasinghe, R., Muis, S., Nicholls, R. J., Lincke, D., & Hinkel, J. (2020). Projections of global-scale extreme sea levels and resulting episodic coastal flooding over the 21st Century. *Scientific Reports*, *10*(1), 11629. https://doi.org/10.1038/s41598-020-67736-6
Kumbier, K., Carvalho, R. C., Vafeidis, A. T., & Woodroffe, C. D. (2018). Investigating compound flooding in an estuary using hydrodynamic modelling: A case study from the Shoalhaven River, Australia. *Natural Hazards and Earth System Sciences*, *18*(2), 463–477. https://doi.org/10.5194/nhess-18-463-2018
Kumbier, K., Carvalho, R. C., & Woodroffe, C. D. (2018). Modelling hydrodynamic impacts of sea-level rise on wave-dominated Australian estuaries with differing geomorphology. *Journal of Marine Science and Engineering*, *6*(2), 66. https://doi.org/10.3390/jmse6020066
Kupfer, S. (2025). Compound flooding—Hydrographs and adaptation measures [Dataset]. *figshare*. https://doi.org/10.6084/m9.figshare.26099137.v1
Kupfer, S., MacPherson, L. R., Hinkel, J., Arns, A., & Vafeidis, A. T. (2024). A comprehensive probabilistic flood assessment accounting for hydrograph variability of ESL events. *Journal of Geophysical Research: Oceans*, *129*(1), e2023JC019886. https://doi.org/10.1029/2023JC019886
Kupfer, S., Santamaria-Aguilar, S., van Niekerk, L., Lück-Vogel, M., & Vafeidis, A. T. (2022). Investigating the interaction of waves and river discharge during compound flooding at Breede Estuary, South Africa. *Natural Hazards and Earth System Sciences*, *22*(1), 187–205. https://doi.org/10.5194/nhess-22-187-2022
Lesser, G. R., Roelvink, J. A., van Kester, J. A. T. M., & Stelling, G. S. (2004). Development and validation of a three-dimensional morphological model. *Coastal Engineering*, *51*(8–9), 883–915. https://doi.org/10.1016/j.coastaleng.2004.07.014
LfU-SH. (2024). Hochwasser-Sturmflut-Information: Pegel-Lübeck-Moisling. Retrieved from https://hsi-sh.de/pegel2/pegel.html?mstnr=114461
Louisor, J., Brivois, O., Mouillon, P., Maspataud, A., Belz, P., & Laloue, J.-M. (2022). Coastal flood modeling to explore adaptive coastal management scenarios and land-use changes under sea level rise. *Frontiers in Marine Science*, *9*, 710086. https://doi.org/10.3389/fmars.2022.710086
Lübeck, B. (1966). Bau- und Architekturgeschichte, Stadtentwicklung in Lübeck. Retrieved from https://bekanntmachungen.luebeck.de/dokumente/d/750/inline
Lübeck, H. (2024). Hochwasser—Informationen über Hochwasserstufen und Maßnahmen. Retrieved from https://www.luebeck.de/de/rathaus/verwaltung/feuerwehr/ihre-sicherheit/hochwasser.html
Luijendijk, A. P., Ranasinghe, R., de Schipper, M. A., Huisman, B. A., Swinkels, C. M., Walstra, D. J. R., & Stive, M. J. F. (2017). The initial morphological response of the Sand Engine: A process-based modelling study. *Coastal Engineering*, *119*, 1–14. https://doi.org/10.1016/j.coastaleng.2016.09.005
LvermGEO. (2023). ATKIS®-Digitale Geländemodelle (DGM und bDOM) [Dataset]. Retrieved from https://www.schleswig-holstein.de/DE/landesregierung/ministerien-behoerden/LVERMGEOSH/Service/serviceGeobasisdaten/geodatenService_Geobasisdaten_DGM.html?nn=b7e3eb10-4e7a-4dd0-8caf-a8911c06430a
Lyddon, C. E., Brown, J. M., Leonardi, N., & Plater, A. J. (2020). Sensitivity of flood hazard and damage to modelling approaches. *Journal of Marine Science and Engineering*, *8*(9), 724. https://doi.org/10.3390/jmse8090724
Lyddon, C. E., Brown, J. M., Leonardi, N., Saulter, A., & Plater, A. J. (2019). Quantification of the uncertainty in coastal storm hazard predictions due to wave-current interaction and wind forcing. *Geophysical Research Letters*, *46*(24), 14576–14585. https://doi.org/10.1029/2019GL086123
MacManus, K., Balk, D., Engin, H., McGranahan, G., & Inman, R. (2021). Estimating population and urban areas at risk of coastal hazards, 1990–2015: How data choices matter. *Earth System Science Data*, *13*(12), 5747–5801. https://doi.org/10.5194/essd-13-5747-2021
MacPherson, L. R., Arns, A., Dangendorf, S., Vafeidis, A. T., & Jensen, J. (2019). A stochastic extreme sea level model for the German Baltic Sea coast. *Journal of Geophysical Research: Oceans*, *124*(3), 2054–2071. https://doi.org/10.1029/2018JC014718
MacPherson, L. R., Arns, A., Fischer, S., Méndez, F. J., & Jensen, J. (2023). Bayesian extreme value analysis of extreme sea levels along the German Baltic coast using historical information. *Natural Hazards and Earth System Sciences*, *23*(12), 3685–3701. https://doi.org/10.5194/nhess-23-3685-2023
Maymandi, N., Hummel, M. A., & Zhang, Y. (2022). Compound coastal, fluvial, and pluvial flooding during historical hurricane events in the Sabine–Neches Estuary, Texas. *Water Resources Research*, *58*(12), e2022WR033144. https://doi.org/10.1029/2022WR033144
MELUR. (2022). Generalplan Küstenschutz des Landes Schleswig-Holstein—Fortschreibung. Retrieved from https://www.schleswig-holstein.de/DE/fachinhalte/K/kuestenschutz/Downloads/Generalplan.pdf?__blob=publicationFile&v=3
Merz, B., Elmer, F., & Thieken, A. H. (2009). Significance of "high probability/low damage" versus "low probability/high damage" flood events. *Natural Hazards and Earth System Sciences*, *9*(3), 1033–1046. https://doi.org/10.5194/nhess-9-1033-2009
Moftakhari, H., Schubert, J. E., AghaKouchak, A., Matthew, R. A., & Sanders, B. F. (2019). Linking statistical and hydrodynamic modeling for compound flood hazard assessment in tidal channels and estuaries. *Advances in Water Resources*, *128*, 28–38. https://doi.org/10.1016/j.advwatres.2019.04.009

MUNL, S. H. (2004). Flussgebietseinheit Schlei/Trave Bericht über die Analysen nach Artikel 5 der Richtlinie 2000/60/EG. Retrieved from https://wasserblick.bafg.de/servlet/is/36524/B_Bericht_Schlei_Trave.pdf?command=downloadContent&filename=B_Bericht_Schlei_Trave.pdf

Myhre, G., Alterskjær, K., Stjern, C. W., Hodnebrog, Ø., Marelle, L., Samset, B. H., et al. (2019). Frequency of extreme precipitation increases extensively with event rareness under global warming. *Scientific Reports*, *9*(1), 16063. https://doi.org/10.1038/s41598-019-52277-4

Najafi, H., Shrestha, P. K., Rakovec, O., Apel, H., Vorogushyn, S., Kumar, R., et al. (2024). High-resolution impact-based early warning system for riverine flooding. *Nature Communications*, *15*(1), 3726. https://doi.org/10.1038/s41467-024-48065-y

Narayan, S., Beck, M. W., Reguero, B. G., Losada, I. J., van Wesenbeeck, B., Pontee, N., et al. (2016). The effectiveness, costs and coastal protection benefits of natural and nature-based defences. *PLoS One*, *11*(5), e0154735. https://doi.org/10.1371/journal.pone.0154735

NDR. (2023). Sturmflut an der Ostsee: Alle Berichte auf einen Blick. Retrieved from https://www.ndr.de/nachrichten/schleswig-holstein/Sturmflut-an-der-Ostsee-Alle-Berichte-auf-einen-Blick,sturmflut2076.html

Olbert, A. I., Moradian, S., Nash, S., Comer, J., Kazmierczak, B., Falconer, R. A., & Hartnett, M. (2023). Combined statistical and hydrodynamic modelling of compound flooding in coastal areas—Methodology and application. *Journal of Hydrology*, *620*, 129383. https://doi.org/10.1016/j.jhydrol.2023.129383

Orton, P., Ralston, D., van Prooijen, B., Secor, D., Ganju, N., Chen, Z., et al. (2023). Increased utilization of storm surge barriers: A research agenda on estuary impacts. *Earth's Future*, *11*(3), e2022EF002991. https://doi.org/10.1029/2022EF002991

Pugh, D. (2004). *Changing sea levels: Effects of tides, weather, and climate*. Cambridge University Press.

Reimann, L., Vafeidis, A. T., & Honsel, L. E. (2023). Population development as a driver of coastal risk: Current trends and future pathways. *Cambridge Prisms: Coastal Futures*, *1*, e14. https://doi.org/10.1017/cft.2023.3

Rentschler, J., Avner, P., Marconcini, M., Su, R., Strano, E., Vousdoukas, M., & Hallegatte, S. (2023). Global evidence of rapid urban growth in flood zones since 1985. *Nature*, *622*(7981), 87–92. https://doi.org/10.1038/s41586-023-06468-9

Rutgersson, A., Kjellström, E., Haapala, J., Stendel, M., Danilovich, I., Drews, M., et al. (2022). Natural hazards and extreme events in the Baltic Sea region. *Earth System Dynamics*, *13*(1), 251–301. https://doi.org/10.5194/esd-13-251-2022

Schoonees, T., Gijón Mancheño, A., Scheres, B., Bouma, T. J., Silva, R., Schlurmann, T., & Schüttrumpf, H. (2019). Hard structures for coastal protection, towards greener designs. *Estuaries and Coasts*, *42*(7), 1709–1729. https://doi.org/10.1007/s12237-019-00551-z

Schroder, K., Hummel, M. A., Befus, K. M., & Barnard, P. L. (2022). An integrated approach for physical, economic, and demographic evaluation of coastal flood hazard adaptation in Santa Monica Bay, California. *Frontiers in Marine Science*, *9*, 1052373. https://doi.org/10.3389/fmars.2022.1052373

Schumann, A. (2017). Flood safety versus remaining risks—Options and limitations of probabilistic concepts in flood management. *Water Resources Management*, *31*(10), 3131–3145. https://doi.org/10.1007/s11269-017-1700-z

Serafin, K. A., Ruggiero, P., Parker, K., & Hill, D. F. (2019). What's streamflow got to do with it? A probabilistic simulation of the competing oceanographic and fluvial processes driving extreme along-river water levels. *Natural Hazards and Earth System Sciences*, *19*(7), 1415–1431. https://doi.org/10.5194/nhess-19-1415-2019

Stadtarchiv Lübeck. (1926). Lübeckilches Jahrbuch der väterstädtilchen Blätter. Jahrgang 1925–1926. Retrieved from https://www.stadtarchiv-luebeck.findbuch.net/pics/R._Digitalisate._~9%20Dienstbibliothek._~9.2%20Digitalisierte%20Zeitschriften._~9.2_2%20VBll._~9.2_2_AUGIAS._~9.1_L%20I%2045_1925-1926.pdf

Stadtarchiv Lübeck. (1929). Lübeckilches Jahrbuch der väterstädtilchen Blätter. Jahrgang 1928–1929. Retrieved from https://www.stadtarchiv-luebeck.findbuch.net/pics/R._Digitalisate._~9%20Dienstbibliothek._~9.2%20Digitalisierte%20Zeitschriften._~9.2_2%20VBll._~9.2_2_AUGIAS._~9.1_L%20I%2045_1928-1929.pdf

Sterr, H. (2008). Assessment of vulnerability and adaptation to sea-level rise for the coastal zone of Germany. *Journal of Coastal Research*, *24*(2), 380–393. https://doi.org/10.2112/07A-0011.1

Sutton-Grier, A. E., Wowk, K., & Bamford, H. (2015). Future of our coasts: The potential for natural and hybrid infrastructure to enhance the resilience of our coastal communities, economies and ecosystems. *Environmental Science and Policy*, *51*, 137–148. https://doi.org/10.1016/j.envsci.2015.04.006

Tebaldi, C., Ranasinghe, R., Vousdoukas, M., Rasmussen, D. J., Vega-Westhoff, B., Kirezci, E., et al. (2021). Extreme sea levels at different global warming levels. *Nature Climate Change*, *11*(9), 746–751. https://doi.org/10.1038/s41558-021-01127-1

Temmerman, S., Horstman, E. M., Krauss, K. W., Mullarney, J. C., Pelckmans, I., & Schoutens, K. (2023). Marshes and mangroves as nature-based coastal storm buffers. *Annual Review of Marine Science*, *15*(1), 95–118. https://doi.org/10.1146/annurev-marine-040422-092951

Toimil, A., Losada, I. J., Nicholls, R. J., Dalrymple, R. A., & Stive, M. J. F. (2020). Addressing the challenges of climate change risks and adaptation in coastal areas: A review. *Coastal Engineering*, *156*, 103611. https://doi.org/10.1016/j.coastaleng.2019.103611

Torres, J. M., Bass, B., Irza, N., Fang, Z., Proft, J., Dawson, C., et al. (2015). Characterizing the hydraulic interactions of hurricane storm surge and rainfall–runoff for the Houston–Galveston region. *Coastal Engineering*, *106*, 7–19. https://doi.org/10.1016/j.coastaleng.2015.09.004

UNESCO WHC. (2022). *Interactive map—UNESCO*. World Heritage Centre. Retrieved from https://whc.unesco.org/en/interactive-map/

vanden Hurk, B. J. J. M., White, C. J., Ramos, A. M., Ward, P. J., Martius, O., Olbert, I., et al. (2023). Consideration of compound drivers and impacts in the disaster risk reduction cycle. *IScience*, *26*(3), 106030. https://doi.org/10.1016/j.isci.2023.106030

Vollstedt, B., Koerth, J., Tsakiris, M., Nieskens, N., & Vafeidis, A. T. (2021). Co-production of climate services: A story map for future coastal flooding for the city of Flensburg. *Climate Services*, *22*, 100225. https://doi.org/10.1016/j.cliser.2021.100225

Völz, V., Hinkel, J., Kupfer, S., MacPherson, L. R., & Wulff Norrby, C. J. (2024). Learning about sea level rise uncertainty improves coastal adaptation decisions. *Earth's Future*, *12*(10), e2024EF004704. https://doi.org/10.1029/2024EF004704

Vousdoukas, M. I., Mentaschi, L., Voukouvalas, E., Verlaan, M., Jevrejeva, S., Jackson, L. P., & Feyen, L. (2018). Global probabilistic projections of extreme sea levels show intensification of coastal flood hazard. *Nature Communications*, *9*(1), 1–12. https://doi.org/10.1038/s41467-018-04692-w

Ward, P. J., de Moel, H., & Aerts, J. C. J. H. (2011). How are flood risk estimates affected by the choice of return-periods? *Natural Hazards and Earth System Sciences*, *11*(12), 3181–3195. https://doi.org/10.5194/nhess-11-3181-2011

WSA. (2022). WSA Ostsee—Startseite. Retrieved from https://www.wsa-ostsee.wsv.de/Webs/WSA/Ostsee/DE/1_Startseite/startseite_node.html

Zscheischler, J., Westra, S., van den Hurk, B. J. J. M., Seneviratne, S. I., Ward, P. J., Pitman, A., et al. (2018). Future climate risk from compound events. *Nature Climate Change*, *8*(6), 469–477. https://doi.org/10.1038/s41558-018-0156-3